EUROPEAN ORGANIZATION FOR NUCLEAR RESEARCH
Laboratory for Particle Physics

CUDI: A MODEL FOR CALCULATION OF ELECTRODYNAMIC AND THERMAL BEHAVIOUR OF SUPERCONDUCTING RUTHERFORD CABLES

A.P. Verweij

CUDI is the extended Fortran code to calculate the electrodynamic and thermal behaviour of any type of Rutherford cable subject to global and/or local variations in field, transport current, and external heat release. The internal parameters of the cable can be freely varied along the length and across the width, such as contact resistances, critical current, cooling rates etc. In this way, all the typical non-uniformities occurring in a cable, e.g. broken filaments, strand welds, cable joints, and edge degradation can be simulated. Also the characteristics of the strands in the cable can be varied from strand to strand. Heat flows through the matrix, through the interstrand contacts, and to the helium are incorporated, as well as the self-field and self- and mutual inductances between the strands. The main features and structure of the program will be discussed.

CERN, Accelerator Technology Department, Geneva, Switzerland

1. Introduction

Modelling of the electrodynamic behaviour of Rutherford cables dates back to the early 1970s. Initially the modelling was focussed on the calculation of the inter-strand coupling currents (ISCCs) and coupling loss in case of a changing external (applied) field. First analytical calculations of these coupling currents were performed by Wilson in the case of unsaturated strands for fields parallel as well as perpendicular to the large face of the cable [1]. In this approach the cable was considered as a solid strip, in which wires spiral uniformly, an approach also followed by Walters and Krempasky [2], [3].

In 1973 Morgan suggested calculating the ISCCs by modelling a Rutherford-type cable as a network of nodes interconnected by strands and cross-contact resistances R_c [4]. Such a discrete approach is more appropriate since the cable has a limited number of strands linked to each other through contact resistances with a spatial distribution. This network model could be applied to cables with unsaturated strands and with constant R_c and field-sweep rate perpendicular to the large cable face. The same type of network model is applied in 1980 to calculate the ISCCs for the ISABELLE cable [5]. Since 1988 other network models have been developed [6, 7, 8, 9, 10, 11, 12], that could also handle saturated strands, adjacent contact resistances R_a and field changes parallel to the large cable face. Later a full electrodynamic network model was developed, including as well the self-field, self- and mutual inductances, longitudinal fields, and possibilities for spatial variations in field, field sweep rate, contact resistances, and critical current [13]. Such local non-uniformities are likely to be present in many cables; for example, partial or complete strand breakage and filament damage in the cable edges due to the cabling process. Using this network model also the existence of Boundary Induced Coupling Currents has been demonstrated [14], as well as the sinusoidal field pattern these currents create in accelerator magnets wound with Rutherford cables.

Also other numerical models on often simplified structures of a Rutherford cable have been developed in recent years in order to study specific characteristics of the cable, such as Minimum Quench Energy (see for example [15]) or so-called 'ramp-rate limitation effects' (see for example [16]).

This paper describes the extension of a complete network model [13] with a thermal module, including heat flows along the strand, towards crossing strands, towards adjacent strands, and towards the helium. The result is a complete Thermal and Electrodynamic Network Model, called CUDI, that can be used to calculate many relevant effects in a Rutherford cable, such as inter-strand coupling currents, boundary-induced coupling currents, inter-strand and inter-filament coupling loss, current distribution, self fields, quench energy, stability, temperature margin, and UI-relation. User friendly interfaces are added to the program for entering the input parameters and visualisation of the results, and a copy of the program is now freely available.

Sections 2 and 3 deal with the geometry of a fully transposed Rutherford-type cable and how this geometry is modelled by means of a three-dimensional network of nodes, interconnected by resistances and strand sections. The equations that are used to solve the unknown currents are given in the next section. The thermal part of the model is discussed in section 5 and in section 6 it is shown how both the electrodynamic and thermal models are integrated, and which algorithm is used to obtain the solution for currents and temperatures. Section 7 concludes by giving an overview of the various input parameters, showing that the flexibility of the network model approach makes it possible to calculate with one model all relevant situations that can occur in a real cable.

2. Cable geometry

The *x-y-z* coordinate system is given in Fig 1. The Rutherford cable with length L_{cab} is situated in the positive *x-y* quadrant and extends in the positive *z*-direction, with a transport current flowing in the *z*-direction of the cable. Also the direction of the self-field (for positive transport current) is shown.
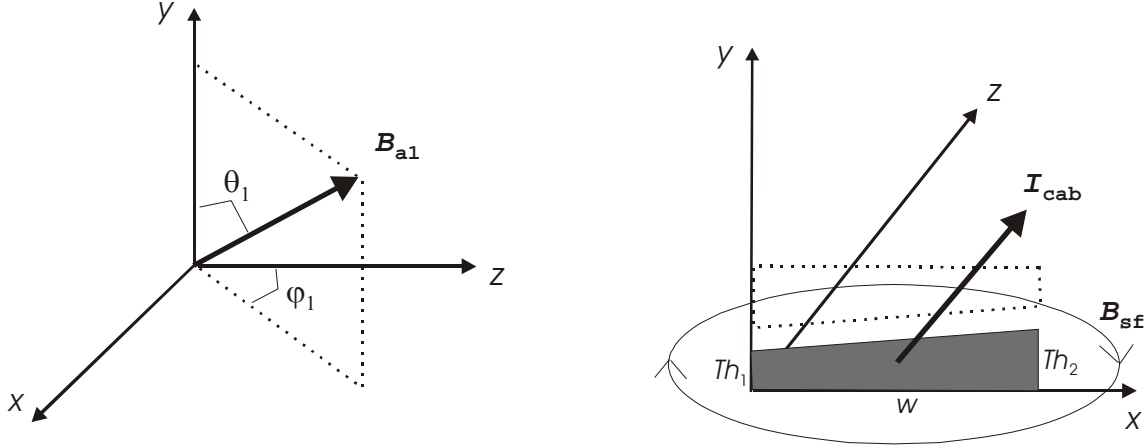

Fig 1.   *x-y-z* coordinate system and definition of the applied field B_{a1}, cable transport current I_{cab} and self field B_{sf}. The dotted cable contour represents the optional return lead.

Two fields can be applied (B_{a1} and B_{a2}) each with their own longitudinal distribution and direction given by:

$$B_{a1,x}(z)=B_{a1}(z)\sin(\theta_1)\sin(\varphi_1) \qquad [T] \tag{1}$$

$$B_{a1,y}(z)=B_{a1}(z)\cos(\theta_1) \quad [T] \tag{2}$$

$$B_{a1,z}(z)=B_{a1}(z)\sin(\theta_1)\cos(\varphi_1) \qquad [T] \tag{3}$$

The three field components are also referred to as the parallel, perpendicular and longitudinal field components respectively. Field B_{a2} is defined in a similar way using the angles θ_2 and φ_2. The cable has a width *w* and a thickness Th_1 on edge 1 and Th_2 on edge 2, and consists of N_S strands, having a twist pitch L_P. A keystone can be implemented by choosing $Th_1 \neq Th_2$. The mid-thickness of the cable is given by $Th_{av}=(Th_1+Th_2)/2$.

A 'return lead' can be added in order to take into account the self field generated by the other cable in a bi-filary cable sample geometry. The transport current in the return lead is opposite to the one in the simulated cable, and is assumed to be uniformly distributed among the strands. No coupling currents are present in the return lead. The return lead is oriented with opposite keystone with respect to the simulated cable (see Fig. 1). Additional stabilizer on the outside of the cable, for example in Rutherford cables with an aluminium jacket, is not taken into account. However its additional current carrying capacities and heat capacity can be handled in CUDI by artificially increasing the matrix volume of the wires, an approach which is probably valid if the electrical and thermal contact between the strands and the jacket is very good.

3. Electrodynamic network model of a Rutherford-type cable

The cable is modelled by a three-dimensional network of nodes interconnected by strand sections and resistances (see Fig. 2). The strands are represented by lines with an infinitely small diameter. This implies that the distance between the line currents at both edges is equal to $w(1-2/N_S)$ and the distance between the line currents in both layers varies between $Th_1/2$ and $Th_2/2$. At both edges of the cable the strands follow a skew path from one layer to the other. At edge 1 the strands go from the upper layer to the lower layer; at edge 2 the strands go from the lower layer to the upper layer. The length of each strand section is about $L_P/(2N_S)$ except for the two sections at the edges that are twice as long. The resistances R_a and R_c represent the resistances between adjacent and crossing strands. A few of these resistances are shown in the figure.
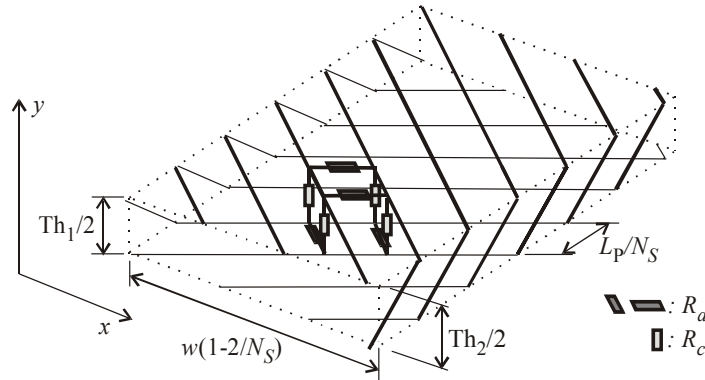

Fig. 2. Network representation of the electrodynamic model of a Rutherford cable, showing for one calculation cell the contact resistances R_a and R_c. Note that the strand resistance R_s and the self- and mutual inductances are not shown.

The currents I_a and I_c are the (coupling) currents between the strands of the cable through the contact resistances R_a and R_c, which can have various spatial distributions, see section 6. The currents I_s are the currents in the strands. A given strand section i has a resistance R_s^i, an inductance M^{ii}, and mutual inductances M^{ij} with all the other j strand sections of the cable. The length of the cable is defined by the number of bands N_B. Each band corresponds to a part of the cable equal to L_P/N_S (see Fig. 3). The start of band 1 is positioned at $z=0$. The end of band N_B is positioned at $N_B L_P/N_S$, which is equal to the cable length L_{cab}.
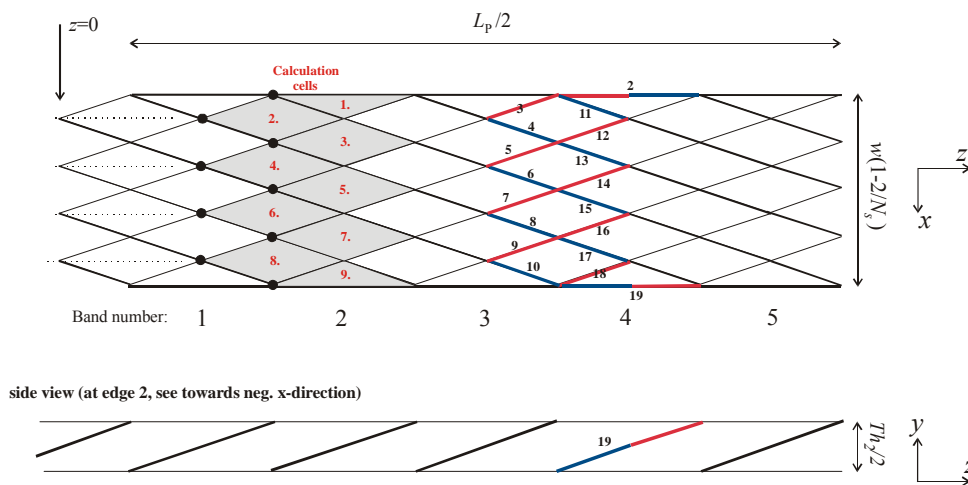

Fig. 3. Longitudinal representation of the 10-strand cable, showing the band numbering, the calculation cells (from 1 to 9), and the numbering of the strand sections (from 2 to 19).

Each band consists of (N_s-1) calculation cells (see Fig. 3) and has ($5N_s$-3) unknown currents, namely:

- ($2N_s$-2) strand currents I_s,
- $2N_s$ currents between adjacent strands I_a,
- (N_s-1) currents between crossing strands I_c.

Note that the small sides of a band consists of four resistances R_a (numbers 1, 2, $2N_s$-1 and $2N_s$) but only two strand elements (numbers 2 and $2N_s$-1), which are about twice as long as the other strand elements.

4. Equations to solve the currents in the network model

Using Kirchhoff's laws the ($5N_s$-3) equations, needed to solve the current distribution in one band, can be set up. The following symbolic notations demonstrate the implementation in the computer code. The ($5N_s$-3) equations consist of:

- ($2N_s$-2) equations in the nodes:
$$\sum I_a + \sum I_c + \sum I_s = 0 \quad [A] .$$
(4)

- ($3N_s$-2) equations for a circuit:
$$\sum (I_a R_a) + \sum (I_c R_c) + \sum U_s = \frac{dB_{\perp A}}{dt} A \quad [V] ,$$
(5)

with $dB\perp_A/dt$ the component of dB/dt normal to the enclosed surface A of the circuit, and U_s the voltage over a strand section. Note that the field is composed of the applied fields B_{a1} and B_{a2} and the self field B_{SF}.

- One constraint:
$$\sum I_a + \sum I_s = I_{cab} \quad [A] ,$$
(6)

stating that all the currents flowing through the cross-section of the cable add up to the cable transport current I_{cab}.

The voltage U_s over a strand section consists of a resistive part U_R and an inductive part U_{ind}. Two types of transitions are implemented in CUDI, namely:

- The power law:
$$U_R = U_C (I_s / I_{crit})^n \quad [V] ,$$
(7)

with U_C the voltage at the critical current I_{crit}. Small and large n-values indicate a gradual and sharp transition respectively.

- A linear increase in the voltage for strand currents larger than I_{crit} assuming that the surplus current (I_s-I_{crit}) flows through the resistive matrix, so that:

$$U_R = 0 \quad [V] \qquad\qquad \text{for } I_s < I_{crit} ,$$
(8a)

$$U_R = R_{mat}(I_s - I_{crit}) \quad [V] \qquad\qquad \text{for } I_s > I_{crit} ,$$
(8b)

with R_{mat} the resistance of the magnetoresistive matrix:

$$R_{\mathrm{mat}}(B) = \rho_{\mathrm{mat}}(B) \frac{l_s}{(1-\eta)\pi d_s^2 / 4} \quad [\Omega] , \tag{9}$$

with l_s the length of the strand section, d_s the strand diameter, ρ_{mat} the field-dependent resistivity of the matrix and η the volume fraction of superconductor in the strand.

The inductive part of the voltage of strand section i is given by:

$$U_{\mathrm{ind}}^i = \sum_{j=1}^{N} M^{i,j} \frac{dI_s^j}{dt} \quad [\mathrm{V}] , \tag{10}$$

with $M^{i,j}$ the mutual inductance between strand sections i and j. The expression of the mutual induction between two wires of finite length placed in arbitrary positions, as given by Grover [17], is used in CUDI. The summation has to be made over all the strand sections of all the bands, so $N=(2N_S-2)N_B$.

Simulation of time-dependent effects is performed at discrete time steps t_m. The time derivative of the strand current is therefore represented by the difference in current between two time steps (t_m and t_{m-1}), with $\Delta t_m = t_m - t_{m-1}$:

$$\frac{dI_s}{dt} = \frac{I_s(t_m) - I_s(t_{m-1})}{\Delta t_m} \quad [\mathrm{As^{-1}}] . \tag{11}$$

Eq. 5 can then be rewritten as:

$$\sum (I_a R_a) + \sum (I_c R_c) + \sum (I_s R_s) + \frac{1}{\Delta t_m} \sum_{j=1}^{N} \left(M^{i,j} I_s^j(t_m) \right) =$$

$$\frac{B_{\perp A}(t_m) - B_{\perp A}(t_{m-1})}{\Delta t} + \frac{1}{\Delta t_m} \sum_{j=1}^{N} \left(M^{i,j} I_s^j(t_{m-1}) \right) \quad [\mathrm{V}] . \tag{12}$$

using $R_s = U_R / I_s$. The right-hand side of this equation is now known except for the (usually very small) time derivative of the self field (since the field is composed of the applied fields and self field).

Boundary currents have to be defined for the first band and the last band. Defining all strand currents equal to 0 A is equivalent to a case without transport current, for example simulating a piece of cable placed in an alternating field in order to measure the AC losses. Defining all strand currents equal to I_{cab}/N_S is equivalent to the case with a uniform joint resistance to the current lead. A non-uniform joint resistance can be simulated by defining different strand currents in the first and last bands.

5. The thermal model

The discretisation of the cable for the thermal model is the same as for the electrodynamic model, i.e. the strands are divided in sections with a length equal to $l_s = L_P/(2N_S)$, except for the two edge sections that are twice as long (see section 3). Contrary to the electrodynamic model, the strand sections in the thermal model have a given volume $V_s = l_s \pi d_s^2 / 4$, with d_s the strand diameter. So for most Rutherford cables, the typical discretisation volume is about 1 mm³. The assumption is made that the material properties, temperature, heating and cooling are uniform over this volume, which is in first approximation correct, especially for strands having a matrix with high thermal conductivity. For a single strand section a thermal model can be set up considering that the section is in direct thermal contact with the helium and the following five strand sections (see Fig. 4):

- Two neighbouring sections (with temperatures T_{n1} and T_{n2}) of the same strand, with a contact area A_{str}, and a heat conductivity $k_{str}(T)$ usually dominated by the heat conductivity of the matrix.
- Two sections of adjacent strands (with temperatures T_{a1} and T_{a2}) , with a contact area A_{adj}, and a heat conductivity $k_{adj}(T)$ dominated by the contact surface, as shown later on.
- One section of the crossing strand (with temperature T_{cr}), with a contact area A_{cross}, and a heat conductivity $k_{cross}(T)$ which is also dominated by the contact surface.
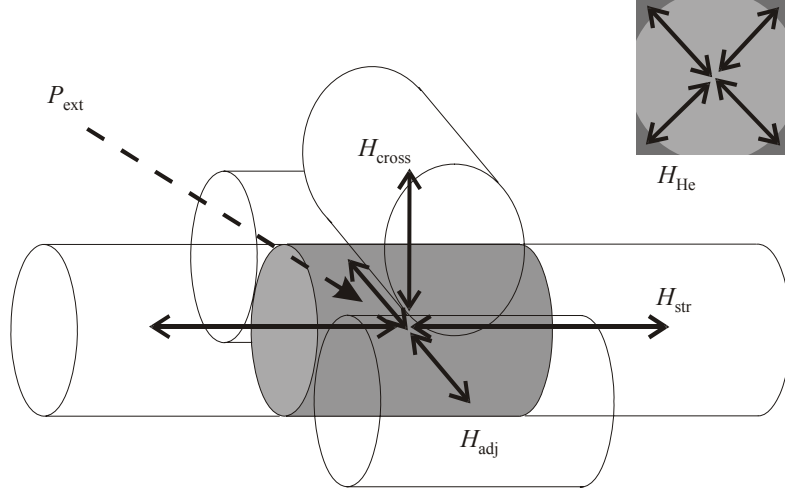

Fig. 4. Model of the thermal heat flows towards one strand section, with heat flows H_{adj} to adjacent strands, H_{cross} to the crossing strand, H_{str} along the same strand, and H_{He} to the helium. The external heat input is represented by P_{ext}.

The contact surfaces A_{adj} and A_{cross} are a function of the cable geometry and vary over the width of the cable due to the cable keystone. Empirical data are available [18] on a few cables which are used to scale to other type of Rutherford cables. A given helium volume (V_{He}) is attributed to each strand section, which is for typical insulated cables about 5-10% of the strand volume V_s. Heat flow is possible between this helium volume and the strand section, but no heat flow is possible between different helium volumes. During the simulation it is assumed that the mass of helium in contact with each strand section remains unchanged, and that its temperature and pressure can vary.

During a time step $\Delta t = t_m - t_{m-1}$, the temperature of the strand section will change by a factor ΔT_s and the temperature of the helium volume by a factor ΔT_{He}. The heat balance for the strand section can then be written as:

$$V_s C_{p,s} \Delta T_s / \Delta t = P_{adj}/4 + P_{cross}/4 + P_s + P_{ext} - H_{str} - H_{adj} - H_{cross} - H_{He} \tag{13}$$

with P_{adj} the resistive heat in R_a, P_{cross} the resistive heat in R_c, P_s the resistive heat in the strand, P_{ext} the externally applied heat, H_{str} the heat flow to the neighbouring strand sections, H_{adj} the heat flow to the adjacent strand sections, H_{cross} the heat flow to the crossing strand section, and H_{He} the heat flow to the helium. Note the factor 4 in Eq. (13) resulting from the fact that the heat that is generated in R_a and R_c is distributed over 4 different strand sections, as can be seen in Fig. 2.

The heat balance for the helium volume attached to each strand section reads:

$$V_{He} C_{v,He} \Delta T_{He} / \Delta t = H_{He} = h_{He} A_{He} \tag{14}$$

with A_{He} the surface in contact with the helium. Note that also V_{He} and A_{He} vary across the cable width for keystoned cables. Adiabatic cases can be studied by defining $h_{He} = V_{He} = 0$, whereas open-bath cases can be simulated with $V_{He} = \infty$ and $\Delta T_{He} = 0$.

6

The heat capacity of the strand is given by:

$$C_{p,s}=\eta C_{p,SC}+(1-\eta)C_{p,mat} \tag{15}$$

with η the filling factor, $C_{p,SC}=f(B, T, I_{crit})$ the heat capacity of the superconductor, and $C_{p,mat}=f(B, T)$ the heat capacity of the matrix. Accurate relations for $C_{p,SC}$, and $C_{p,mat}$ are incorporated in CUDI for standard materials such as NbTi, Nb$_3$Sn and Cu, as well as the heat capacity for helium at constant volume.

The heat flow terms to the 5 other strand sections can be written as:

$$H_{str}=k_{str}(T_s-T_{n1})A_{str}/l_s+k_{str}(T_s-T_{n2})A_{str}/l_s \tag{16}$$

$$H_{adj}=k_{adj}(T_s-T_{a1})A_{adj}+k_{adj}(T_s-T_{a2})A_{adj} \tag{17}$$

$$H_{cross}=k_{cross}(T_s-T_{cross})A_{cross} \tag{18}$$

The longitudinal heat conduction in the strand is usually dominated by the matrix; e.g. the heat conductivity of copper is about 400 W/K/m, whereas for NbTi it is about 4 orders of magnitude smaller. Data for k_{str} are incorporated in CUDI for standard materials such as NbTi, Nb$_3$Sn and Cu.

The conductivity between two adjacent strands (k_{adj}) can be written in first approximation by:

$$k_{adj}=k_{cont}*k_{str}/(k_{cont}+k_{str}/d) \tag{19}$$

with d the strand diameter, and k_{cont} the heat conductivity of the contact between the two strand surfaces (in W/K/m^2), given by:

$$k_{cont}=xT^q \tag{20}$$

with typical values for x of 100-1000 W/m^2/K$^{(1+q)}$ and q=1.5-2.5 [19], depending on the oxidation level of the strand surface. Using these values and taking k_{str}=400 W/K/m, d=10^{-3} m, and T=4 K, it is immediately clear that $k_{str}/d>>k_{cont}$ so that $k_{adj}=k_{cont}*d$, i.e. the thermal resistance is dominated by the contact surface. Only at much higher temperatures will k_{str} start to play a role. Similar equations can be set up for the heat conduction to the crossing strand.

In CUDI the steady-state heat flow to boiling Helium I is defined by 3 regimes:

Natural convection: $\quad h_{He}=c_1(T_s-T_{He})\quad\quad$ for $h_{He}<h_{He}{}^*$ $\tag{21a}$

Nucleate boiling: $\quad h_{He}=c_2(T_s-T_{He})^{2.5}\quad$ for $h_{He}{}^*<h_{He}<h_{He}{}^{**}$ $\tag{21b}$

Film boiling: $\quad h_{He}=c_3(T_s-T_{He})\quad\quad$ for $h_{He}>h_{He}{}^{**}$ $\tag{21c}$

where the parameters c_1, c_2, c_3, $h_{He}{}^*$ and $h_{He}{}^{**}$ can be freely varied. Typical values are 500 Wm^{-2}K^{-1}, $5\cdot10^4$ Wm^{-2}K$^{-2.5}$, 250 Wm^{-2}K^{-1}, 10 Wm^{-2}, and 10^4 Wm^{-2} respectively [20,21]. A transient cooling regime, preceding the steady-state regimes, is defined by:

Kapitza regime: $\quad h_{He}=c_4(T_s{}^4-T_{He}{}^4)\quad\quad$ for $\int_{t0}^{t} h_{He}(t)dt < q_{lim,I}$ $\tag{21d}$

where the parameters c_4 and $q_{lim,I}$ can be varied by the user. This transient regime is present until the cumulative heat transfer from the conductor exceeds the critical energy $q_{lim,I}$ (in Wm^{-2}). A typical value for c_4 is 100-300 Wm^{-2}K^{-1}, depending on the surface coating and oxidation of the strand [22].

The steady-state heat flow to subcooled Helium II is described by the following formulas:

Kapitza regime: $\quad h_{He}=c_5(T_s{}^p-T_{He}{}^p)\quad\quad$ for $T_s-T_{He}<T^*$ $\tag{22a}$

7

Film boiling: $\qquad h_{\mathrm{He}}=c_6(T_{\mathrm{s}}-T_{\mathrm{He}}) \qquad$ for $T_{\mathrm{s}}-T_{\mathrm{He}} > T^*$ (22b)

where the parameters c_5, c_6, p and T^* can be varied by the user. Typical values for c_5 and p are 100-1000 $Wm^{-2}K^{-p}$ and 1-4 respectively, depending on the surface condition of the strand. In transient mode the Kapitza regime is present until the cumulative heat transfer from the conductor exceeds the critical energy $q_{lim,II}$ (which is also a parameter that can be varied by the user). Note that there are various formulas in literature defining the limiting energies $q_{lim,I}$ and $q_{lim,II}$ depending on the type of helium channels in the cable, and the heat flux. It is very likely that the real heat transfer from a strand towards the helium does not exactly follow the above given relations in all situations. Comparison between experimental data and calculated values, which is foreseen in the coming years, can possibly give better insight in the heat transfer.

During the time step Δt the temperature of the strand and the helium can change considerably, and hence also the values of the critical current, strand resistance, and resistive powers. All terms in the heat balance equations are therefore averaged over the time Δt; for example, the heat capacity of the matrix is a function of both the temperature at the previous time step and the actual time step, so $C_{\mathrm{p,mat}}=f(T_{\mathrm{s}}(t_{\mathrm{m-1}}), T_{\mathrm{s}}(t_{\mathrm{m}}))$.

6. Solving algorithm

Calculations are performed for any pattern in time of the applied field(s), transport current and external heat release. The time steps have to be defined by the user and the code will iteratively calculate for each time step the solution of currents and temperatures everywhere in the cable. At each time step a matrix with dimensions $N_{\mathrm{B}}(5N_{\mathrm{S}}-3)$ by $N_{\mathrm{B}}(5N_{\mathrm{S}}-3)+1$ is set up, containing all the relations of eqs. (4)-(6). Many matrix components contain the resistance R_{s}, which is a function of the current I_{s}, the critical current $I_{\mathrm{crit}}(B, T)$, and hence also of the strand temperature T_{s}. The solution of the currents and temperatures requires therefore an iterative algorithm with the temperature module nested inside the electrodynamic module, as briefly described in the following way (with the temperature module in bold):

Estimate initial values for the currents and temperatures, based on the solution of previous time steps and on the increase in field and transport current of the actual time step.
LOOP
    Calculate the self-field based on the calculated currents of previous iterations.
    Calculate the resistances R_{s} based on the calculated currents and critical currents of previous iterations.
    Calculate the powers based on the calculated currents and resistances R_{s} of previous iterations.
        LOOP
            LOOP
                Find the solution of Eqs. (13) and (14) using the most recently calculated temperatures of the other strand sections
            UNTIL (the T_{s} and T_{He} of one section have converged to the required accuracy)
        UNTIL (all temperatures of all sections in the cable have converged to the required accuracy)
    Calculate $I_{\mathrm{crit}}=f(B, T_{\mathrm{s}})$ and $R_{\mathrm{s}}=f(I_{\mathrm{s}}, I_{\mathrm{crit}})$ with the most recently calculated values of T_{s} and I_{crit}
    Solve the matrix and obtain new values for I_{a}, I_{c} and I_{s}.
UNTIL (all currents have converged to the required accuracy)

Note that the initial estimate of the expected currents and temperatures (before the outer iteration loop starts) is quite important, since a good estimate can reduce the number of iterations considerably, whereas a bad estimate can sometimes even lead to non-convergence. The inner loop requires an iterative approach not only because of the very non-linear behaviour of the relations for heat capacity, heat conductivity, and heat flow to helium, but also because all terms in the heat balance equations are averaged over the time Δt, and therefore also depend on the solution of currents and temperatures of the actual time step. The central loop is needed because all temperatures of the cables depend on each other through the thermal heat flows H_{adj}, H_{cross}, and H_{str}. The required accuracies are typically 10^{-3} A for the currents and 10^{-4} K for the temperatures.

Different cases can now be distinguished:
1. Constant temperature and all currents much smaller than the critical current. In this case, $\Delta T_s=\Delta T_{He}=0$ and $U_R=R_s=0$, so that the temperature module is not used and the unknown currents I_a, I_c and I_s are calculated by solving the matrix only once, if the effect of the self-field can be neglected. A few iterations of the outer loop may be needed if the self-field is not negligible.
2. Constant temperature and one or more currents close to or larger than the critical current. In this case, $\Delta T_s=\Delta T_{He}=0$ so that the temperature module is not used. In the transition R_s becomes a function of I_s and I_{crit} and the unknown currents I_a, I_c and I_s have to be calculated by iteration through the outer loop. The convergence speed depends strongly on the steepness of the transition, the values of the contact resistances, time step and ramp rate of the transport current.
3. Variable temperature and all currents much smaller than the critical current, implying of course as well that all temperatures remain below the critical temperature. In this case the currents and temperatures can be solved independently. The temperatures are solved through iteration of the central and inner loops. Convergence speed depends strongly on the temperature, helium flow regime, time step and heating powers. The currents are solved in the same way as for case 1).
4. Variable temperature and one or more currents close to or larger than the critical current. In this case R_s is also a function of the critical current and hence of the temperature. Furthermore, the temperature is a function of the heating, the cooling and the heat capacities and hence a function of the currents I_a, I_c and I_s (i.e. the solution of the matrix), and the temperatures T_s and T_{He} (i.e. the solution of the heat balance equations). Convergence speed now strongly depends on the steepness of the transition, the values of the contact resistances, time step, ramp rate of the transport current, temperature, helium flow regime, and heating powers. Currents and temperatures can in some cases not converge at all, especially if the time steps are badly defined by the user. In this case the program will add automatically intermediate time steps so that temperature and current variations are smaller, and the initial estimate of currents and temperatures is more precise.

In order to reduce the computing time, especially for long cables, the mutual inductances are included only for strand sections spaced apart by less than $N_{B,mut}$ bands (where $N_{B,mut}$ can be set by the user). By doing so the matrix will contain large areas of zeros in the lower left and upper right areas (see Fig. 5, matrix A), and computing time will be reduced significantly. Another advantage is that the equations in the square matrix A can be rewritten into a rectangular matrix B, which strongly reduces the use of internal memory. Only taking into account part of the mutual inductances is surely valid if the time derivative of the applied field is much larger than that of the self-field, because the twist of the strands reduces the inductive coupling. However, for a relatively large changing self-field, the transposition has basically no effect on the reduction of the coupling, and a large value for $N_{B,mut}$ could be required. In the latter case a good and faster alternative is by using a small $N_{B,mut}$ and calculating all the currents by solving the matrix iteratively, where the inductive component of the sections that are

far away are added to the right hand side of eq. (12). Convergence is usually fast because this inductive component has only a minor effect on the current distribution.
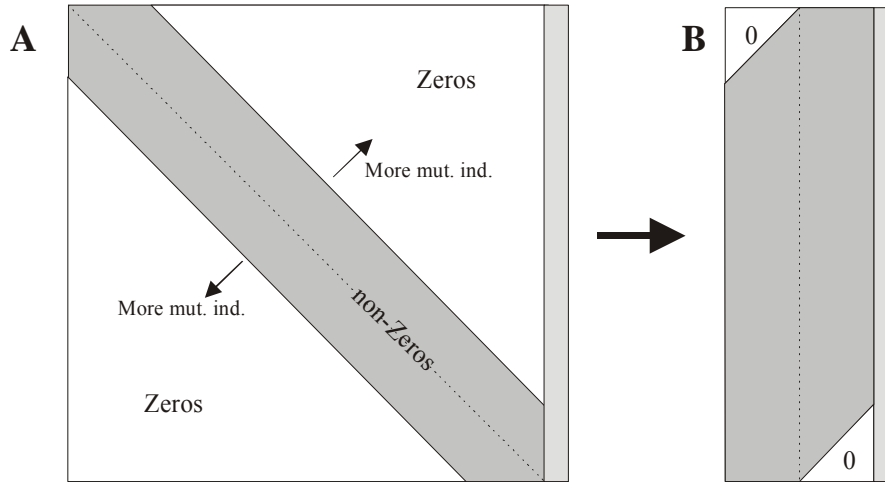

Fig. 5.   Effect of the use of $N_{B,mut}$ on the number of zeros in the matrix. By neglecting the mutual inductances between strand sections that are spaced far away, one can rewrite matrix A into matrix B, thereby reducing the use of internal computer memory.

7. Conclusions

With the recent implementation of a thermal module, a complete code, called CUDI, is now available for calculation of electrodynamic and thermal effects in Rutherford cables. Any type of Rutherford cable geometry can be simulated, including cables with partially superconducting and partially normal conducting strands. The additional stabilizer of jacketed Rutherford cables is not taken into account, although its additional current carrying capacity and heat capacity can be handled in CUDI by artificially increasing the matrix volume of the wires. The critical current, *n*-value, *RRR*, and contact resistance can be defined per strand, which is realistic since the wires of a multi-strand cable are often not made in the same production batch, and hence have slightly different characteristics. Any type of $I_{crit}(B, T)$ surface can be defined, as well as any type of relation for the SC-to-normal transition. Furthermore, many parameters can be varied along the length of the cable, to take into account realistic field maps and variations in contact resistances due to variation in pressure, soldering etc. Resistances R_a and R_c can also be varied across the width, which is likely to occur in keystoned cables, and can be given additional random distributions. Resistive cores/barriers can be simulated by increasing R_c in the cable centre. Also local variations in critical current and contact resistance can be programmed, in order to simulate, for example, current degradation in the cable edges (due to the cabling process), cold welds, broken strands, punch-throughs of the core etc.

Calculations are performed for any pattern in time of the applied field(s), transport current and external heat release. The transport current at the ends of the cable can be set uniform or non-uniform, simulating homogeneous respectively non-homogeneous joints with the current leads. The time steps have to be defined by the user and the code will iteratively calculate for each time step the solution of currents and temperatures everywhere in the cable. Calculation of the actual iteration step takes into account the results of temperatures and currents found in previous iteration steps, so as to converge faster to the required accuracy. Convergence is usually rather fast if the temperature rise is negligible or if the currents are smaller than the critical current. However, calculations in the resistive transition

along with a temperature variation can converge slowly or in some cases not converge at all, especially if the time steps are badly defined by the user. In the latter case the program will add automatically intermediate time steps so that temperature and current variations are smaller and give automatically a more stable iteration process.

A free public version of the code is available, together with a user friendly input module and a special routine for visualization of the output data. The electrodynamic part of the program was validated in the past, see especially [13], mainly by means of measurements on cables and magnets of inter-strand and boundary-induced coupling currents and their characteristic times. The thermal part of the program is not yet validated. For adiabatic conditions (e.g. in case of impregnated cables) the simulations are very likely to be correct. However, the simulation of the heat exchange with helium in the thermal module of the program is probably still too simple. At present, the program assumes 1) fixed helium volumes 'attached' to each strand section, 2) no helium flow between different helium volumes, and 3) no heat transfer between different helium volumes. Stability measurements on Rutherford cables at 1.9 K and 4.3 K with external heat pulses are currently performed to compare CUDI calculations with experimental data.

References

[1] Wilson MN. Rate dependent magnetization in flat twisted superconducting cables. RHEL int. note M-A-26, 1972.

[2] Walters CR. Magnetization and design of multistrand superconducting conductors. IEEE Trans Magn 1975;11:328-331.

[3] Krempasky L. AC losses in flat twisted superconducting cables. CERN int. note SPS/EA/78-2, 1978.

[4] Morgan GH. Eddy currents in flat metal-filled superconducting braids. J Appl Phys 1973;44:3319-3322.

[5] Courant ED. Eddy currents in superconducting braid. ISABELLE Technical note 168, 1980.

[6] Sytnikov VE, et al. Coupling losses in superconducting transposed conductors located in changing magnetic fields. Cryogenics 1989;29:926-930.

[7] Sytnikov VE, et al. Transport and induced currents distribution in superconducting transposed cables. Adv Cryog Eng 1992;38:553-558.

[8] Sytnikov VE, Peshkov IB. Coupling losses for superconducting cables in pulsed fields. Adv Cryog Eng 1994;40: 537-542.

[9] Niessen EMJ, et al. Application of the network method to superconducting cables. in: Proc. LTEC 90, p. 5.4, 1990.

[10] Niessen EMJ, Van de Klundert LJM. Loss calculations for the 29-strand NET braid. University of Twente, Int. note UTNET90.2, 1990.

[11] Niessen EMJ. Continuum electromagnetics of composite superconductors. PhD thesis, University of Twente, The Netherlands, 1993.

[12] McDonald J. Description of the Network Model for Rutherford-Type Cables. Fermilab Technical Document TD-04-017, 2004.

[13] Verweij AP. Electrodynamics of Superconducting Cables in Acclerator Magnets, PhD thesis, University of Twente, The Netherlands, 1995.

[14] Verweij AP. Modelling Boundary-Induced Coupling Currents in Rutherford-type Cables. IEEE Trans on Appl SC 1997:723-726.

[15] Wilson MN, Wolf R. Calculation of Minimum Quench Energies in Rutherford Cables. IEEE Trans on Appl SC 1997:950-953.

[16] Krempasky L, Schmidt C. Ramp-rate limitation in large superconducting magnets due to supercurrents. Cryogenics 1996;36:471-483.

[17] Grover FW. Inductance calculations – working formulas and tables. Dover Publications, New York, 1946, p. 55.

[18] Depond JM, et al. Examination of Contacts between Strands by Electrical Measurement and Topographical Analysis. IEEE Trans on Appl SC 1997;7:793-796.

[19] Nilles MJ, Van Sciver SW. Effects of Oxidation and Roughness on Cu Contact Resistance from 4 K to 290 K. Adv Cryog Eng (Materials) 1988;34, Plenum Press.

[20] Schmidt C. Review of steady state and transient heat transfer in pool boiling helium I. in: Stability of Superconductors, 1981, p. 17, Internat. Inst. of Refrig. Comission A, Saclay, France.

[21] Van Sciver SW. Helium cryogenics. Plenum Press, NY, 1986.

[22] Kashani A, Van Sciver SW. High heat flux Kapitza Conductance of Technical Copper with several different Surface Preparations. Cryogenics 1985;25:238.